CBPF-NF-083/96

Bogomolny Section for the Stadium. I. Quantum Theory

by

J.S.Espinoza Ortiz[*] *and A.M. Ozorio de Almeida*

Centro Brasileiro de Pesquisas Físicas - CBPF
Rua Dr. Xavier Sigaud, 150
22290-180 – Rio de Janeiro, RJ – Brazil

[*]Instituto de Física
UNICAMP, C.P. 6165
13083-970 – Campinas, SP, Brazil

Abstract

The quarter-stadium can be decomposed into a rectangle and a quarter-circle; in each of these the Helmholtz equation is separable. We thus construct Green functions for both regions and a fully quantum mechanical Bogomolny matrix. There results a very efficient algorithm for calculating eigenvalues and eigenfunctions. We discuss the relation of the family of periodic 'bouncing ball' orbits to the contribution of the non-oscillating modes.

1 Introduction

The study of quantum systems by means of surfaces of section can be quite as illuminating as that of classical systems. This is specially evident where the semiclassical limit is concerned, since the approximate Green function obtained by Bogomolny (1990,1992) for the quantum section depends directly on the classical orbits that intersect the corresponding Poincaré section. Even within a full quantum theory, the interpretation of Doron and Smilansky (1992), further developed by Prosen (1996), provides an intuitive decomposition of bound motion into the scattering from both sides of the Bogomolny section.

Strictly, the physical scattering only occurs for the finite number of propagating modes, i.e., open channels to the left and to the right of the section. Besides these, there is a discrete infinity of evanescent modes which must be taken into account for exact quantization. Even though these modes are included in the unitary operator of Prosen (1996) they do not correspond to classical motion and are therefore not accounted for in Bogomolny's semiclassical propagator. Suppose, then, that we translate or rotate the section so as to loose a significant component of the classical motion; to be specific, a set of short periodic orbits no longer crosses the section. The construction of scattering channels will be insensitive to this alteration, while the semiclassical propagator will be essentially affected. We conclude that the contribution of the non-oscillating modes must be enhanced relatively to the propagating modes which alone contribute to the semiclassical limit.

The study of the simple case of separable systems by Ozorio de Almeida (1994) revealed explicitly that classical motion that does not intersect the Bogomolny section affects the quantization condition through the non-oscilating modes. Of course, separable systems are a tool for the study of the present formalism, rather than the reverse. More interesting is the investigation by Prosen (1996) of semiseparable systems, i.e., systems that are separable on either side of the section, though the whole system is not. The classical dynamics is then nontrivial, containing a generic mixture of regular and chaotic motion. Another semiseparable system is the quarter-stadium. By placing the Bogomolny section as in Fig. 1, we divide it into a rectangle and a quarter-circle.

The purpose of this paper is to study the quantum mechanics of the quarter-stadium from the point of view of this particular Bogomolny section. It is already of interest just to note that one of the few paradigmatic models of fully chaotic systems can be exactly

decomposed into alternating forms of separable motion both in classical and in quantum mechanics. Another feature of interest is that the marginally stable bouncing ball family of periodic orbits shown in Fig. 1 does not cross the section, so we can investigate how this affects the evanescent contributions to the energy eigenvalues and the corresponding eigenstates. It is specially interesting to discuss the relation between our exact results with those of Tanner (1996) who uses the same section for the semiclassical Green function.

It is curious that the usual scattering quantization scheme is not convenient for the present system. The rectangle in Fig. 1 can be easily joined to a semi-infinite tube to the right of the section. However, though we could also join the quarter-circle to a similar tube on the left, the resulting system would not be separable, so that the individial modes would not satisfy the boundary conditions. It is much better to take advantage of the lattitude in the original construction of Bogomolny (1992) to obtain a Green function on the right on a separable basis as explained by Ozorio de Almeida (1994). This can also be interpreted as a nonphysical scattering in an infinitely winding tube, rather than a linear tube.

The construction of the Bogomolny Green function is presented in section 2. The contribution of the non-oscillating modes is discussed section 3. It is shown that these can only be fully understood by considering the quarter-stadium as the limit of a tube with a bend, such as those treated by Lin and Jaffe (1996). There follows the presentation of numerical results for the eigenvalues and eigenfunctions of the quarter-stadium in section 4. Section 5 concludes with a discussion of the contribution of the evanescent modes and their relation to the bouncing ball orbits. Work is in progress on a second paper where we will discuss the semiclassical limit of our Green function in a sequence of approximations.

2 The Section Green Function

Following Bogomolny (1992), we should construct Green functions $G_1(q, q', E)$ and $G_2(q, q', E)$ in the respective regions of Fig. 1, satisfying the inhomogeneous Helmholtz equation

$$(E - \nabla_q^2) G_j(q, q', E) = \delta(q - q') \ , \tag{1}$$

where q is the position (x, y). Furthermore, G_1 should satisfy the same Dirichlet boundary condition as the eigenfunctions of the quarter-stadium along the horizontal radius and the

quarter-circle in Fig. 1, whereas G_2 is cancelled along the sides of the rectangle (2), except for the section itself.

Separability in both regions leads to explicit formulae for the Green functions in terms of the spectral decompositon in eigenmodes, just as obtained by Ozorio de Almeida (1994). The simplest is region (2), where we decompose

$$G_2(q,q';E) = \sum_m g_2(x,x';k_m^2)\langle y|2,m\rangle\langle m,2|y'\rangle \ , \tag{2}$$

where, $k_m^2 = E - m^2\pi^2$, and

$$\langle m,2|y\rangle = \langle y|2,m\rangle = \sqrt{2}\ \sin m\pi y \tag{3}$$

and we choose the Green function for the one-dimensional x-motion to be

$$g_2(x,x';k_m^2) = \frac{1}{k_m}\ \exp[\imath k_m(x'+a)]\sin k_m(x+a) \quad , \quad (x \le x') \ . \tag{4}$$

This is not the only possibility for a Green function that satisfies the boundary conditions in region (2), but it was shown by Ozorio de Almeida (1994) to be one that avoids spurious zeroes in the eigenvalue condition. It is obtained by taking the image of the source at x' with respect to $x = -a$, so that the quantum motion corresponds to two paths between x' and x. One is direct, while the other path bounces off $x = -a$. Therefore this choice is related to the scattering formalisms of Doron and Smilansky (1992) and Prosen (1996): there is never a possibility for the motion to return, once it leaves region (2).

Bogomolny's hypothesis that we can represent any wave function in region (2) as

$$\psi_2(x,y) = \int_0^1 dy'\mu_2(y')G_2(x,y,0,y';E) \ , \tag{5}$$

reduces to

$$\psi_2(x,y) = \sum_m \mu_{2m} g_2(x,0;k_m^2)\langle m,2|y\rangle \ , \tag{6}$$

where

$$\mu_{2m} = \int dy'\mu_2(y')\langle y'|2,m\rangle \ , \tag{7}$$

because of separability. Since the $\langle m,2|y\rangle$ form a complete basis for the Hilbert space of functions on the section, the representation (6) is always feasible.

We can also separate the Helmholtz equation in region (1), using polar coordinates: $q = (r, \phi)$, obtaining

$$\frac{d^2}{d\phi^2}\ F(\phi) + \nu^2 F(\phi) = 0\ , \tag{8}$$

which has the same form as the separate equation for x in region (2), and Bessels' equation,

$$\left[\frac{\partial}{\partial r}\left(r\ \frac{\partial}{\partial r}\right) + Er - \frac{\nu^2}{r}\right]\langle r|1\rangle = 0\ . \tag{9}$$

The situation is different from that discussed by Ozorio de Almeida (1994), because the Bogomolny section is now a radius, rather than the arc of a circle. Hence the modes are determined by the condition that $\langle r = 0|1\rangle = \langle r = 1|1\rangle = 0$, so that

$$\langle n, 1|r\rangle = \langle r|1, n\rangle \propto J_{\nu_n}(kr)\ , \tag{10}$$

where $k = \sqrt{E}$ and the sequence of real numbers ν_n is determined by the equation

$$J_{\nu_n}(kr)\ |_{r=1} = 0\ . \tag{11}$$

The integer n determines the number of nodes in $\langle r|1, n\rangle$, just as m lables $\langle y|1, m\rangle$. For small n, $J_{\nu_n}(kr)$ will not resemble the sine functions, but for $kr >> \nu$, we can use the approximation (Abramowitz and Stegun, 1964).

$$J_\nu(kr) \simeq [kr]^{-\frac{1}{2}} \cos[kr - \nu\pi/2 - \pi/4]\ , \tag{12}$$

so that for $n \geq 1$ condition (11) becomes

$$\nu_n(k) = \frac{2k}{\pi} + \frac{1}{2} - 2n \tag{13}$$

in this limit. Thus, when $E >> n$ we obtain $\nu_n \sim \sqrt{E}$, just as $k_m \sim \sqrt{E}$ when $E >> m$.

The Green function for the one-dimensional angular motion can now be chosen, in exact analogy to (4), as

$$g_1(\phi, \phi'; \nu_n^2) = \frac{1}{\nu_n}\ \exp\left[\imath\nu_n\left(\frac{\pi}{2} - \phi'\right)\right]\sin\nu_n\left(\frac{\pi}{2} - \phi\right)\ ,\ (\phi > \phi') \tag{14}$$

so that the full Green function in region (1) becomes

$$G_1(q, q'; E) = \sum_n g_1(\phi, \phi'; \nu_n^2)\ \langle r|1, n\rangle\langle n, 1|r'\rangle\ . \tag{15}$$

Therefore, G_1 is diagonal in the Bessel, $|1,n\rangle$, representation, just as G_2 is diagonal in the sine-Fourier, $|1,m\rangle$, representation.

We can now also use $\langle r|1,n\rangle$ as an orthogonal basis for the Hilbert space defined on the section, since they are solutions of the Sturm-Liouville problem (9) with Dirichlet boundary conditions (see e.g. Smirnov, 1964). Thus we may decompose any density

$$\mu_1(r) = \sum_n \mu_n \langle n,1|r\rangle \tag{16}$$

and hence obtain any wave function in region (1) in the form

$$\begin{aligned} \psi_1(r,\phi) &= \int_0^1 dr'\ \mu_1(r') G_1(r,\phi,r',0;E)\ ; \\ &= \sum_n \mu_{1n} g_1(\phi,0;\nu_n^2)\ \langle n,1|r\rangle \end{aligned} \tag{17}$$

The wave functions $\psi_1(r,\phi)$ and $\psi_2(x,y)$ (defined by (5) or (6)) satisfy the Helmholtz equation and the boundary conditions in their respective regions. The condition that they should match along the section, together with their normal derivative, is that there exist an unique section density $\mu(y) = \mu_2(y) = \mu_1(r)\ |_{r=y}$, such that

$$\int_0^1 dy\ \mu(y)\tilde{G}(0,y,q'';E) = \int_0^1 dr\ \tilde{G}(q',r,0;E)\mu(r) = 0\ , \tag{18}$$

where

$$\begin{aligned} \tilde{G}(q'',q';E) &= \int_0^1 dy\ \{G_1(r,0,r',\phi';E)|_{r=y} \frac{\partial}{\partial x}\ G_2(x'',y'',0,y;E) \\ &- G_2(x'',y'',0,y;E)\left[\frac{1}{r}\ \frac{\partial}{\partial\phi}\ G_1(r,0,r',\phi';E)\right]_{r=y}\Bigg\}\ , \end{aligned} \tag{19}$$

following Bogomolny (1992) or Ozorio de Almeida (1994). Expanding G_1 in the $\langle r|1,n\rangle$ basis and G_2 in the $\langle y|2,m\rangle$ basis, we obtain

$$\begin{aligned} \tilde{G}(q'',q';E) &= \sum_{nm}\Bigg\{ g_1(0,\phi';\nu_n^2)\ \frac{\partial}{\partial x}\ g_2(x'',0;k_m^2) \int dy \langle m,2|y\rangle\langle y|1,n\rangle \\ &- g_2(x'',0;k_m^2)\ \frac{\partial}{\partial\phi}\ g_1(0,\phi';\nu_n^2) \int \frac{dy}{y}\ \langle m,2|y\rangle\langle y|1,n\rangle\Bigg\} \langle y''|2,m\rangle\langle n,1|r'\rangle\ . \end{aligned} \tag{20}$$

Here, we recognize immediately the matrix elements for exchanging basis. The real matrix $\langle 2|1\rangle$, with elements

$$\langle m,2|1,n\rangle = \int \frac{dy}{y}\ \langle m,2|y\rangle\langle y|1,n\rangle \tag{21}$$

is not unitary or orthogonal, because it transforms eigenfunctions of Sturm-Liouvile operators with different weight functions (Smirnov, 1964):

$$\langle m,2|y\rangle = \sum_n \langle m,2|1,n\rangle\langle n,1|y\rangle \ . \tag{22}$$

Since both sets of basis functions are real, we shall always use $\langle 2|1\rangle$ or $\langle 1|2\rangle$ for the decomposition of sines into Bessel functions:

$$\langle y|2,m\rangle = \sum_n \langle y|1,n\rangle\langle n,1|2,m\rangle \tag{23}$$

represents the same expression as (22). The reverse expansion

$$\langle n,1|y\rangle = \sum_m \langle n,1|2,m\rangle^{-1}\langle 2,m|y\rangle \tag{24}$$

is given by the inverse matrix $\langle 1|2\rangle^{-1} = \langle 2|1\rangle^{-1}$, where

$$\langle 1|2\rangle^{-1}_{nm} = \langle n,1|2,m\rangle^{-1} = \int dy \langle n,1|y\rangle\langle y|2,m\rangle \ . \tag{25}$$

Taking q'' and q' onto the section, we now obtain

$$\tilde{G}(0,y'',0,r';E) = \sum_{nm}\langle y''|2,m\rangle\langle m,2|\tilde{G}|1,n\rangle\langle n,1|r'\rangle \ , \tag{26}$$

where

$$\begin{aligned}\langle m,2|\tilde{G}|1,n\rangle &= \frac{\partial}{\partial x}\, g_2(0,0;k_m^2)\langle m,2|1,n\rangle^{-1} g_1(0,0;\nu_n^2) \\ &- g_2(0,0;k_m^2)\langle m,2|1,n\rangle\, \frac{\partial}{\partial\phi}\, g_1(0,0;\nu_n^2) \ .\end{aligned} \tag{27}$$

Thus the compatibility condition for equations (18), i.e.

$$\sum_m \langle \mu|2,m\rangle\langle m,2|\tilde{G}|1,n\rangle = \sum_n \langle m,2|\tilde{G}|1,n\rangle\langle n,1|\mu\rangle = 0 \ , \tag{28}$$

is that the Bogomolny determinant

$$\det\langle m,2|\tilde{G}|1,n\rangle = 0 \ . \tag{29}$$

From this, we easily derive the eigenvalue condition in terms of the real matrix,

$$\Pi_{mn} = \exp(-\imath k_m a)\langle m,2|\tilde{G}|1,n\rangle \exp\left(-\imath\nu_n\frac{\pi}{2}\right) \ , \tag{30}$$

$$\det \Pi(E) = \det \left\{ \cos k_m a \langle m,2|1,n\rangle^{-1} \ \frac{\sin \nu_n \frac{\pi}{2}}{\nu_n} \ + \frac{\sin k_m a}{k_m a} \langle m,2|1,n\rangle \cos \nu_n \ \frac{\pi}{2} \right\} = 0 \ . \tag{31}$$

Thus the eigenenergies are obtained as the zeroes of a real function.

We see in this formal expression that the cost of using separable bases on each side of the section is that it becomes necessary to use explicitly the non-unitary matrix elements between the sine-Fourier basis and the Bessel basis. Even so we shall show in §4 that (31) supplies an extremely efficient method for calculating energy eigenvalues and eigenfunction. Before this, we must discuss the finite truncation of $\Pi(E)$, which depends on the contribution of the evanescent modes.

3 Non-oscillating modes

The use of $\langle m,2|y\rangle$ as a basis for arbitrary square-integrable functions on the section with Dirichlet boundary conditions prevents any restriction on the integer m. Therefore the transverse wave number k_m will be imaginary for $m \geq \sqrt{E}/\pi$, that is, the corresponding modes will be of the form $\sinh |k_m|(x+a)$, a superposition of exponentially increasing and decreasing modes. The latter, also known as evanescent modes, are the only kind allowed in a semi-infinite tube, because the amplitude must remain finite. For the same reason, the weight of the present non-oscillating modes will decrease rapidly with m even within the finite region for which we defined the Green function $G_2(q,q';E)$.

In the case of completely separable systems, it was shown by Ozorio de Almeida (1994) that non-oscillatory modes do not affect the zeroes of the Bogomolny determinant. Indeed, the matrix $\tilde{G}$ is then diagonal, so that the eigenenergies are obtained from the cancellation of individual matrix elements. The modes of the stadium are strongly coupled, so we cannot in principle ignore those that do not oscillate, though they will not contribute in the semiclassical limit.

We can make a rough evaluation of the strength of the coupling of the non-oscillatory modes in region (2) to the oscillatory modes in region (1) by combining approximations (12) and (13) to obtain

$$J_{\nu_n}(kr) \approx \begin{cases} [kr]^{-\frac{1}{2}} \cos\left[k(r-1)+n\pi-\frac{\pi}{2}\right] & (kr > \nu_n) \\ 0 & (kr < \nu_n) \ , \end{cases} \tag{32}$$

for $n \geq 1$. Therefore, the matrix elements between the Fourier and the Bessel bases will be approximately

$$\begin{aligned} \langle n,1|1,m\rangle^{-1} &\approx \int_{\nu_{n/k}}^{1} dy\ \frac{1}{[\pi k y]^{\frac{1}{2}}} \left\{ \sin\left[(m\pi - k)y + k - n\pi + \frac{\pi}{2}\right] \right. \\ &+ \left. \sin\left[(m\pi + k)y - k + n\pi - \frac{\pi}{2}\right] \right\} \end{aligned} \tag{33}$$

and the maximum contribution occurs for $k = \sqrt{E} = m\pi$, cancelling the oscillations in the first integral, so that, using (13),

$$\langle n,1|2,m\rangle^{-1}_{max} \approx \frac{2}{\pi}\ \frac{(-1)^{m-n}}{\sqrt{m}} \left\{ 1 - \left[\frac{2}{\pi} \left(1 - \frac{n - 1/4}{m} \right) \right]^{\frac{1}{2}} \right\}\ , \tag{34}$$

whereas a similar calculation leads to

$$\langle m,2|1,n\rangle_{max} \approx \frac{(-2)}{\pi}\ \frac{(-1)^{m-n}}{\sqrt{m}}\ \left\{ 1 - \left[\frac{2}{\pi} \left(1 - \frac{n - 1/4}{m} \right) \right]^{-\frac{1}{2}} \right\}\ . \tag{35}$$

The second sine term in (33) falls off faster than (34) by a factor of order $(m\pi + k)^{-1}$, whereas the main term tails off with m as $(m\pi - k)^{-1}$ with respect to (34) or (35).

Thus, we find that the magnitude of the matrix elements are farely insensitive to the index n of the Bessel representation, but there is a maximum for $m = \sqrt{E}/\pi$. Surprisingly this is just the point that separates the oscillating modes from the real exponential modes. Since m must be an integer, we find that the strongest coupling will alternate in energy between the highest oscillating mode and the lowest non-oscillating mode. Though we shall verify numerically that only rarely do the non-oscillating modes affect strongly the values of the eigenenergies, they always contribute an important component to the wave function in region (2).

There must also be an infinite basis in the Bessel representation of functions defined on the section. However, there is a curious anomaly masking the nature of the non-oscillating modes in this case. To understand the problem, it is convenient to consider the quarter-stadium as the limit of the family of billiards sketched in Fig. 2, that is, we substitute the quarter-circle by a quarter-ring in region (1) with inner radius ρ and outer radius $(1 + \rho)$. The Dirichlet boundary conditions on the Bessel equation (9) now lead to a sequence of solutions

$$\langle r|1,n\rangle = \cos\alpha_n J_{\nu_n}(kr) + \sin\alpha_n Y_{\nu_n}(kr)\ , \tag{36}$$

where $Y_\nu(x)$ are real Neumann functions, singular at the origin if k is real. Hence $\alpha_n \to 0$ when $\rho \to 0$.

In the same way as before, n specifies the number of modes in $\langle r|1,n\rangle$, but, since ν_n decreases with n, there is a maximum n for which ν remains real. To obtain further nodes, ν_n must become imaginary, leading to non-oscillating modes in the transverse angular direction. Both $J_\nu(x)$ and $Y_\nu(x)$ are bounded near the origin when ν is imaginary, though both functions oscillate infinitely rapidly as $x \to 0$. By increasing the modulus of ν we can bring in as many modes as we may want from the neighbourhood of the origin into the range between ρ and $(1+\rho)$. However, the sequence of ν_n becomes more closely packed on the origin as ρ is decreased, so that in the limit as $\rho \to 0$, an infinite sequence of imaginary ν_n accumulate at $\nu = 0$.

For the billiard in Fig. 2 with any finite radius ρ, we can add any number of non-oscillating modes to the representation of wave functions in region (1), just as in region (2). This must be truncated, once a numerical convergence of $\det \tilde{G}(E)$ is achieved, because further addition of rows with very small elements to the determinant will eventually lead to numerical instability. This truncation becomes essential in region (1) for the limit $\rho \to 0$, i.e. the quarter-stadium. In this case, we can only take one non-oscillating mode in the quarter-circle, precisely $\nu = 0$, whatever the value of k. This mode will have the form (36) with α_n chosen so as to satisfy the boundary condition at $r = 1$. (Though $Y_0(kr)$ diverges at the origin, all the integrals in the theory are well defined). Hence we place a bound on the dimension of the determinant, though it turns out that this always brings in non-oscillating modes in region (2) so as to complete the square matrix $\langle m|\tilde{G}|n\rangle$.

It is interesting to note that the billiard in Fig. 2 is very similar to the system recently studied by Lin and Jaffe (1996). They also give special consideration to non-oscillating modes, but their problem is to include exponentially increasing modes in open tubes.

4 Numerical Results

The computation of eigenenergies for the quarter-stadium from the real determinant (31), with the dimension of the matrix determined by the number of real ν_n plus the mode ν_0, turns out to be efficient and precise. In Fig. 3 we exhibit the cumulative density of states for the stadium with $a = 1$ and the deviation from the smoothed density including

the Weyl term plus corrections reviewed in Baltes and Hilf, (1976). The effect in the spectrum of excluding the evanescent modes from the Bogomolny matrix is displayed in Fig. 4. Here we find that the deviation is always less than half of the mean level spacing, so that we may assume that the eigenvalues have basically converged in spite of the small size of the matrices used, as shown in Fig. 5.

In Fig. 6 we compare our spectrum with the very precise results calculated by Vergini and Saraceno (1995) using superpositions of plane waves and non-oscillating waves. Again the deviations lie within one third of the averaged level spacing. It is noteworthy that for both methods the intrinsic evaluation of precision is quite different. As in most other cases, Vergini ascertains that the wave intensity at the boundary is close enough to satisfying the Dirichlet boundary conditions. This is automatically satisfied by the Bogomolny method, whereas the difficulty is now with the smoothness of the matching along the section of the wave functions obtained as expansions (6) and (17) shown in Fig. 7. Finally, Fig. 8 exhibits two examples of the Wronskian

$$w(y) = |\psi_1(y,0)\ \frac{\partial}{\partial x}\ \psi_2(0,y) - \psi_2(0,y)\ \frac{1}{y}\ \frac{\partial}{\partial \phi}\ \psi_1(y,0)|\ , \tag{37}$$

whereas the integral of $w(y)$ over the section is shown in Fig. 9. In all cases the wave functions have been previously normalized along the section, that is

$$\int_0^1 |\psi_1(y,0)|^2 dy = \int_0^1 |\psi_2(0,y)|^2 dy = 1\ . \tag{38}$$

5 Discussion

The use of a fully quantum mechanical section for the stadium billiard is an enlightening example of the Bogomolny theory for chaotic motion. The distinctive feature is that all but one member of the family of bouncing ball orbits neither cross nor even touch the chosen section, but this is off-set by the fact that the last of these orbits actually coincides with the section.

Tanner (1996), following Sieber et al. (1993), and Alonso and Gaspard (1994), argues that the bouncing ball orbits can be entirely subtracted from spectrum, because the spectral determinant factors into two parts, one of which is never zero. But this term is essentially that of the Green function for free propagation along the tube. Certainly, the resulting continuous spectrum will not contribute discrete eigenvalues, but the bouncing

ball orbits are not dense within the corresponding classical motion. So we see how difficult it is to attribute parts of the spectrum to specific classical features: changing the boundaries may not alter certain orbits, but it will alter the Green function in which the orbits appear in the semiclassical limit.

It is lucky that the section used by Tanner is close enough to the bouncing balls for their contribution not to relie entirely on evanescent modes, which are absent from the semiclassical approximation employed. Our results in Fig. 4 show that the inclusion of non-oscillating modes only makes a small correction to the eigenvalues. If the section used were a radius within the quarter circle, a series of eigenenergies would be entirely missed within the semiclassical theory. It would be interesting to verify this prediction computationally.

Even so, the evanescent modes provide a significant component to the eigenfunctions dominated by bouncing ball scars such as Fig. 7. These states appear mostly near the quantization condition $k = m\pi$ as expected, though there is a small 'random' component as well. In contrast, the effect of the non-oscillating modes on the energy spectrum near these values is sometimes suppressed, as shown in Fig. 4.

Finally, we note that there exists a remarkable correspondence between the disappearence of exponentially decaying angular modes in the annular region of Fig. 2 with the squeezing out of radial bouncing balls as the inner radius $\rho \to 0$. If we consider the quarter-stadium to arise in this limit, which is necessary for our construction, we obtain two points at which the boundary joins straight lines to circles non-analytically, instead of one. Thus we expect that the mismatch of the wave-functions on both sides of the section shown in Fig. 8 will be a maximum near zero or one, because we are providing analytical expressions on both sides of the section for wave functions that are not analytical at these positons.

Work is now progress to derive Bogomolny semiclassical approximation for the spectrum in terms of classical orbits of the Poincaré map, explicitly from the quantum mechanical spectral determinant for the stadium. This should provide further insight into the dynamics of this paradigmatic model.

Acknowledgements

We thank Dr. R.Vallejos and Dr. R.Ioro for valuable discussions. One of the authors (JSEO) specially acknowledge support from FAPESP (Fundação de Amparo à Pesquisa do Estado de São Paulo), contract number 93/4948-3 .

References

1 Abramowitz M and Stegun A, 1964 Handbook of Mathematical Functions (New York: Dover).

2 Alonso D and Gaspard P, J Phys A 27, 1599 (1994).

3 Baltes HP and Hilf ER, (1978) Spectra of Finite Systems Mannheim: Wissenchaftsverlag.

4 Bogomolny E, 1990 Comments Atomic Molecular Phys 25 67.
Bogomolny E, 1992 Nonlinearity 5 1055

5 Doron E and Smilansky U, Nonlinearity 5, 1055 (1992)

6 Lin K and Jaffe RL, submitted to Physical Review b (November 1995)

7 Ozorio de Almeida AM, J Phys A: Math. Gen 27 (1994) 2891-2904

8 Prosen T, Physica D91 (1996) 244-227

9 Sieberg M, Smilansky U, Creagh SC and Littlejohn RG, J Phys A 26, 6217 (1993)

10 Smirnov VI 1964 A course of Higher Mathematics vol 5 (Oxford Pergamon).

11 Tanner G, Preprint (July 1996).

12 Vergini E and Saraceno M, Phys. Rev E 52, 2204 (1995)

Figure Captions

Figure 1)The stadium billiard constructed as the adition of a rectangle (region(2)) and a quarter of circle (region(1)).The Bogomolny section is defined at $x = 0$ and the vertical lines in region (2) represent the bouncing ball classical orbits.

Figure 2)The family of billiards with inner radius ρ and outer radius $(1 + \rho)$. As in figure (1)the Bogomolny section is defined at $x = 0$.

Figure 3)Figure (3a):The broken lines show the cumulative density of states as a function of the energy; the continuous line shows the smooth Weyl density including corrections, for the stadium billiard with $a = 1$. Figure (3b) shows deviations from the Weyl term.

Figure 4)The efect in the spectrum of excluding the evanescent modes as a function of the wave number $K = \sqrt{2E}$.

Figure 5)The dimension of the matrix $\tilde{\mathrm{G}}$ as function of the wave number $K = \sqrt{2E}$.

Figure 6)Comparing our spectrum (EB) with that of Vergini and Saraceno (EV). In the horizontal axis n represents the sequence of eingenvalues.

Figure 7)The wave function obtained from the expansions (6) and (17). a) K=28.1169 , b) K=25.2175 , c)K=24.3744 , d)K=34.7367 , e)K=27.7044 , f) K=33.8106 , g) K=28.0063 , h)K=26.9704, i) K=32.9431. Here K= $\sqrt{2E}$

Figure 8)Two examples of the Wronskians ($w(y) \geq 0$) at the section. In figure 8a) K=8.8807, $n = 8$, and in figure 8b) K=28.2478, $n = 101$.

Figure 9)Integral of $w(y)$ over the section. The horizontal axis n represents the sequence of eigenvalues.

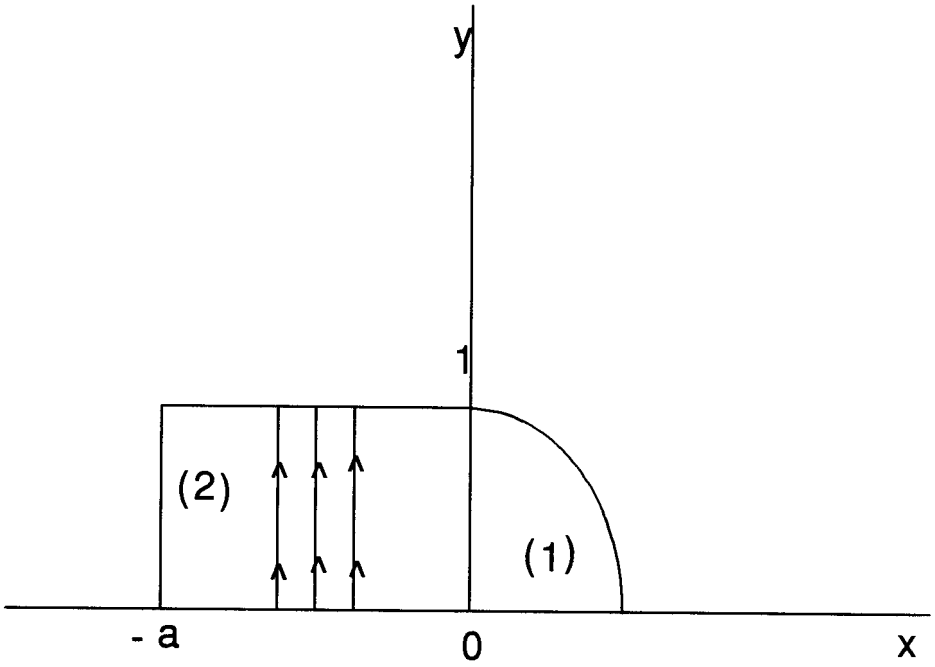

FIG. 1

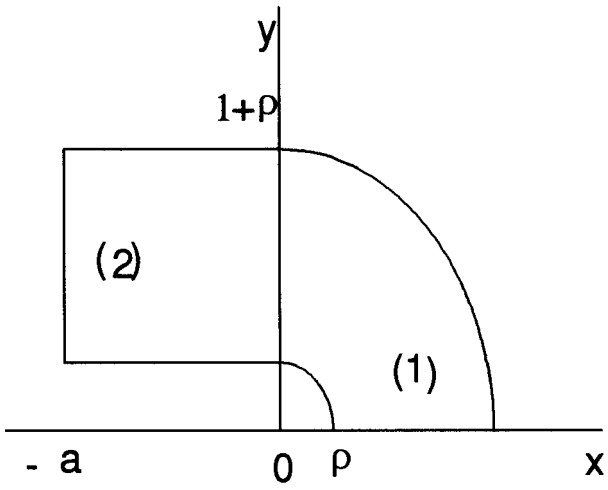

FIG. 2

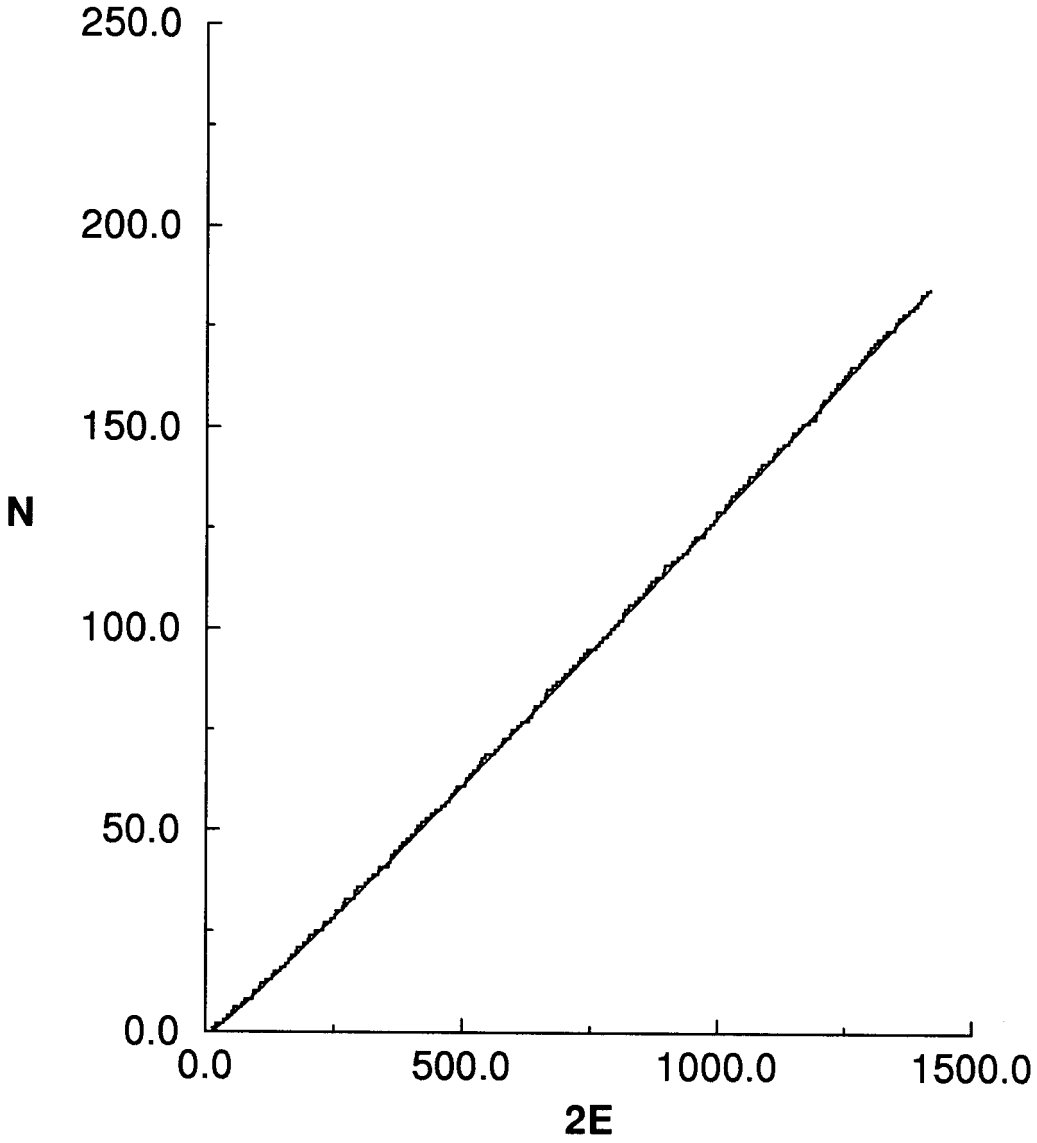

FIG. 3a

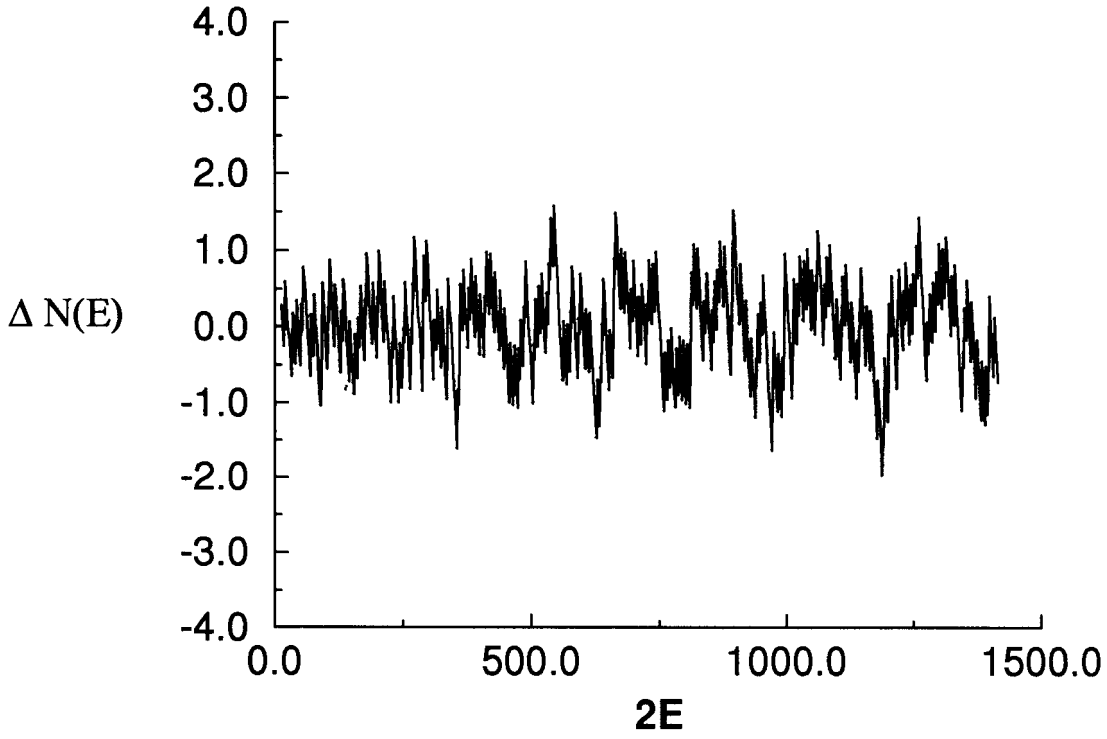

FIG. 3b

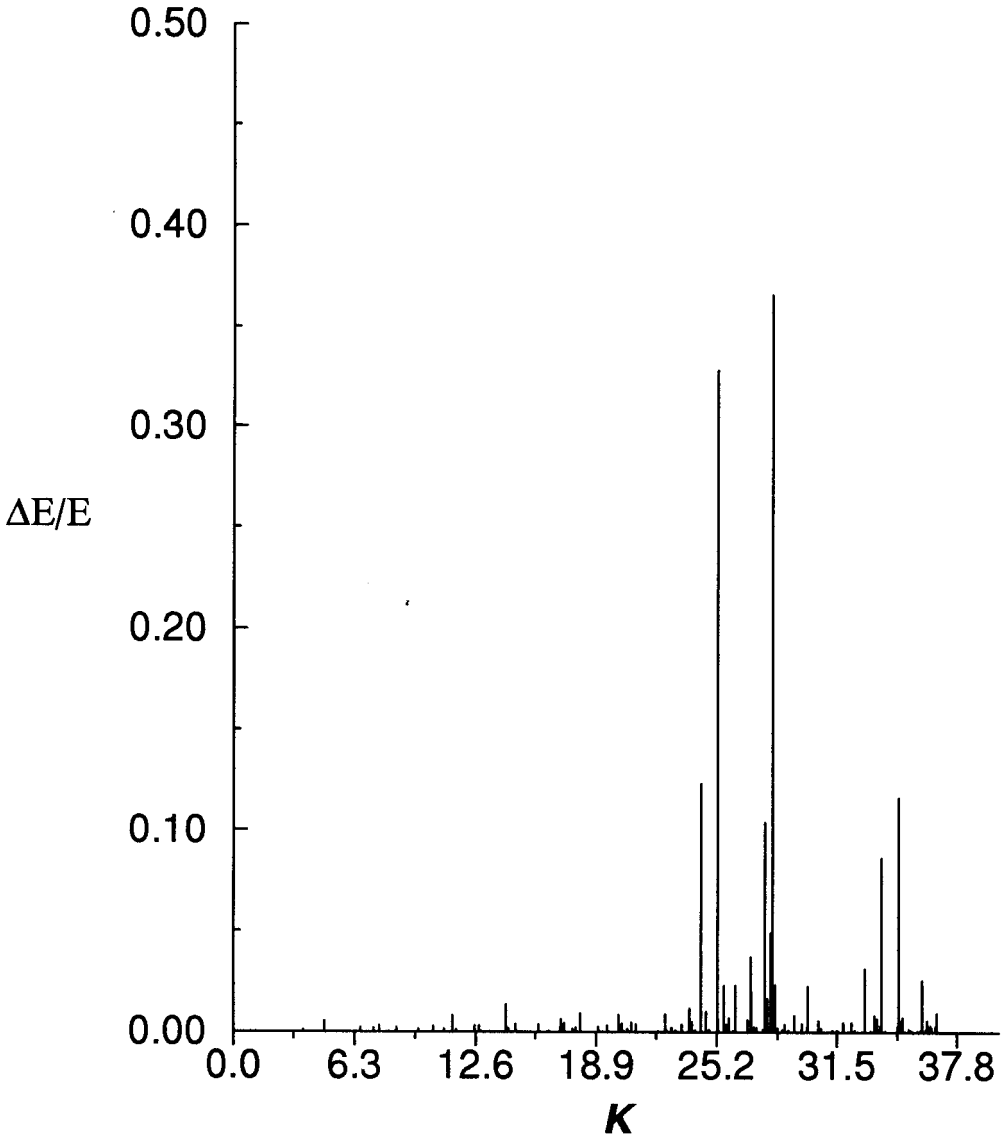

FIG. 4

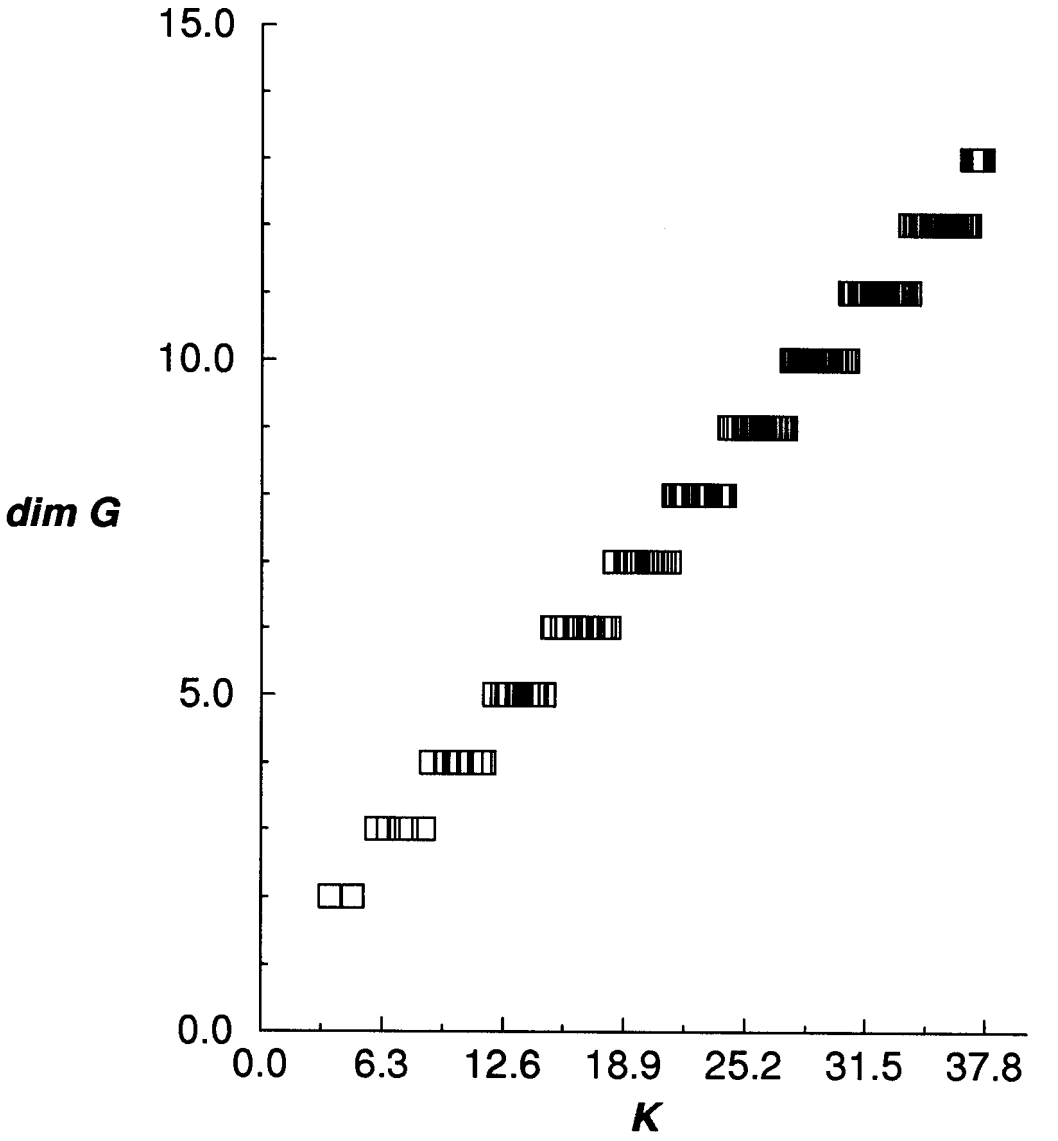

FIG. 5

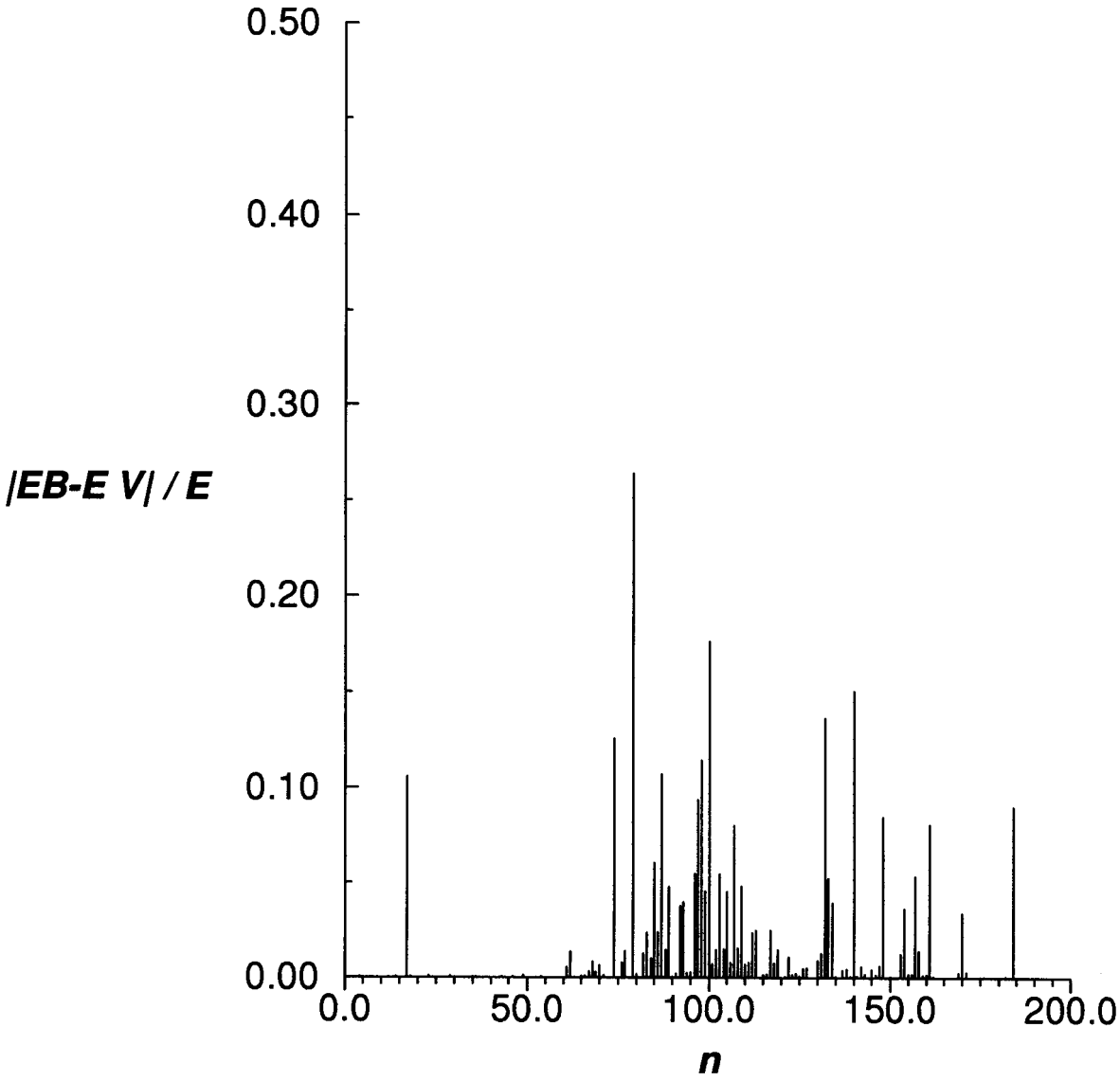

FIG. 6

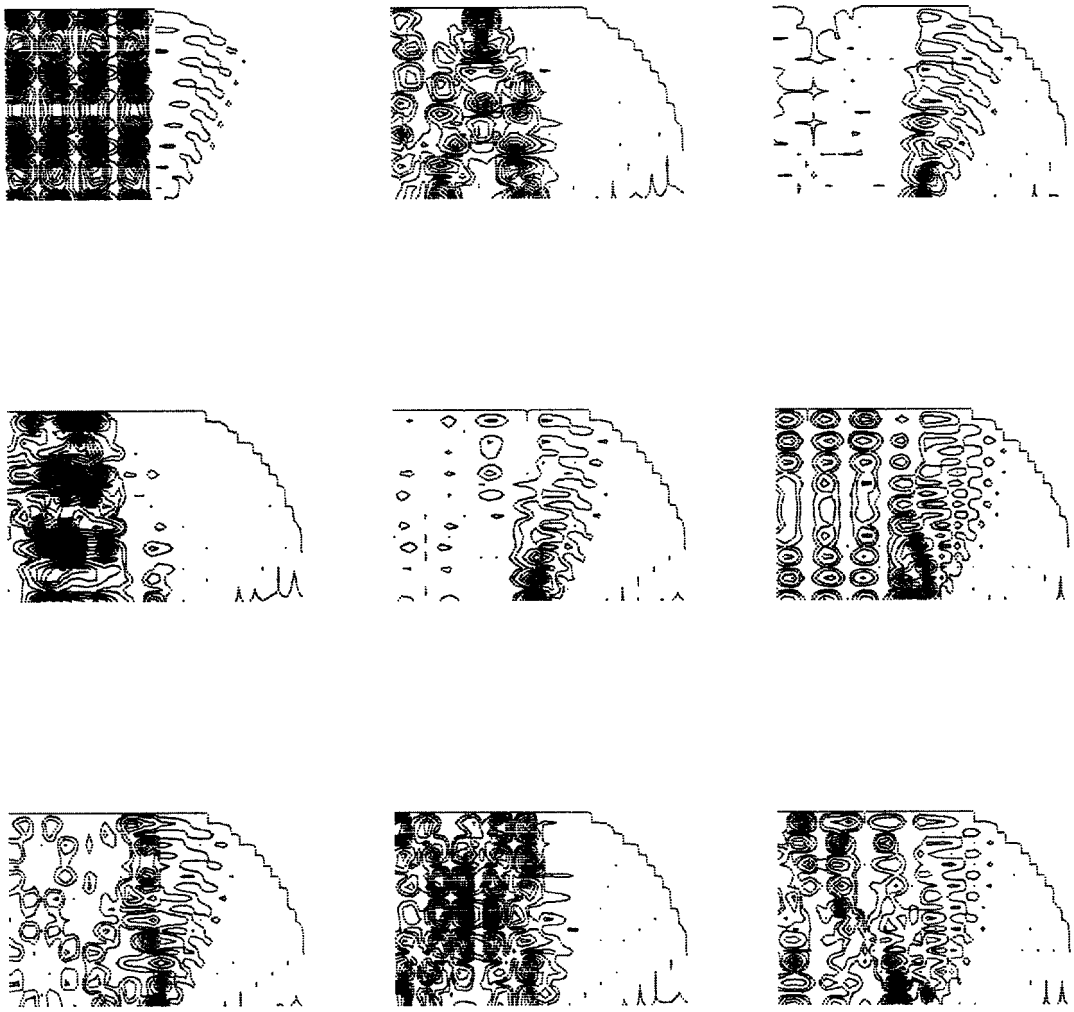

FIG. 7

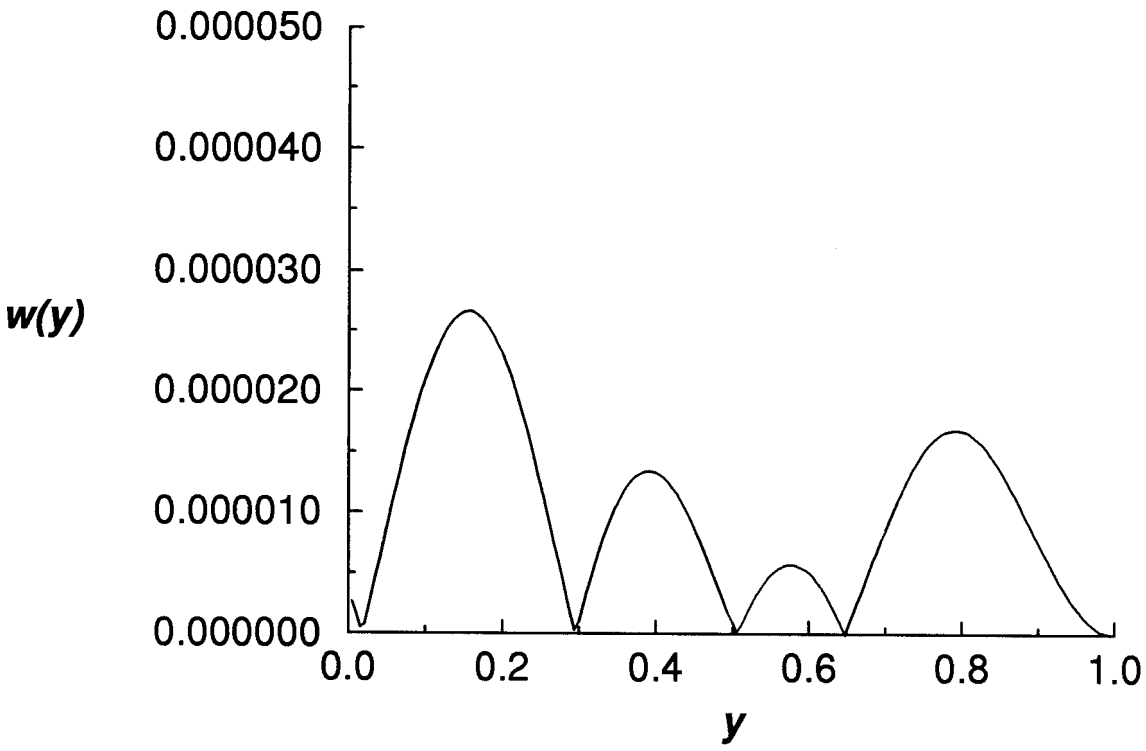
0.000050
0.000040
0.000030
0.000020
0.000010
0.000000
w(y)
0.0
0.2
0.4
0.6
0.8
1.0
y

FIG. 8a

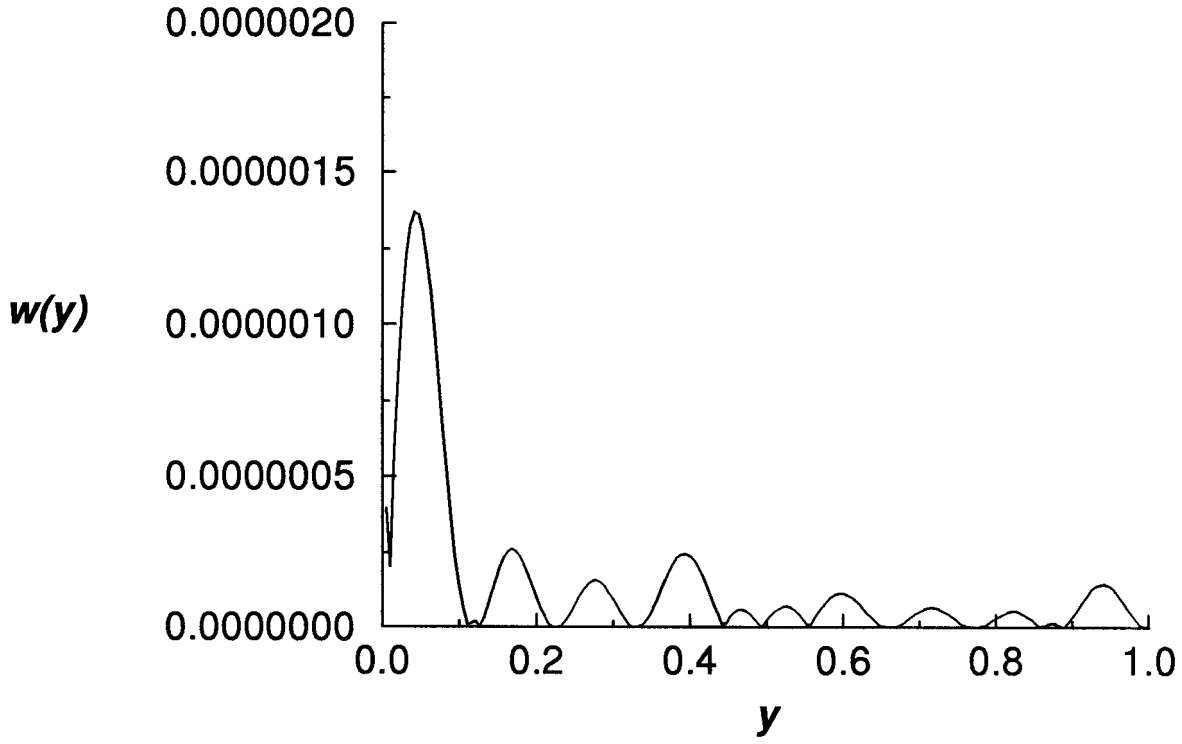
w(y)
0.0000020
0.0000015
0.0000010
0.0000005
0.0000000
0.0
0.2
0.4
0.6
0.8
1.0
y

FIG. 8b

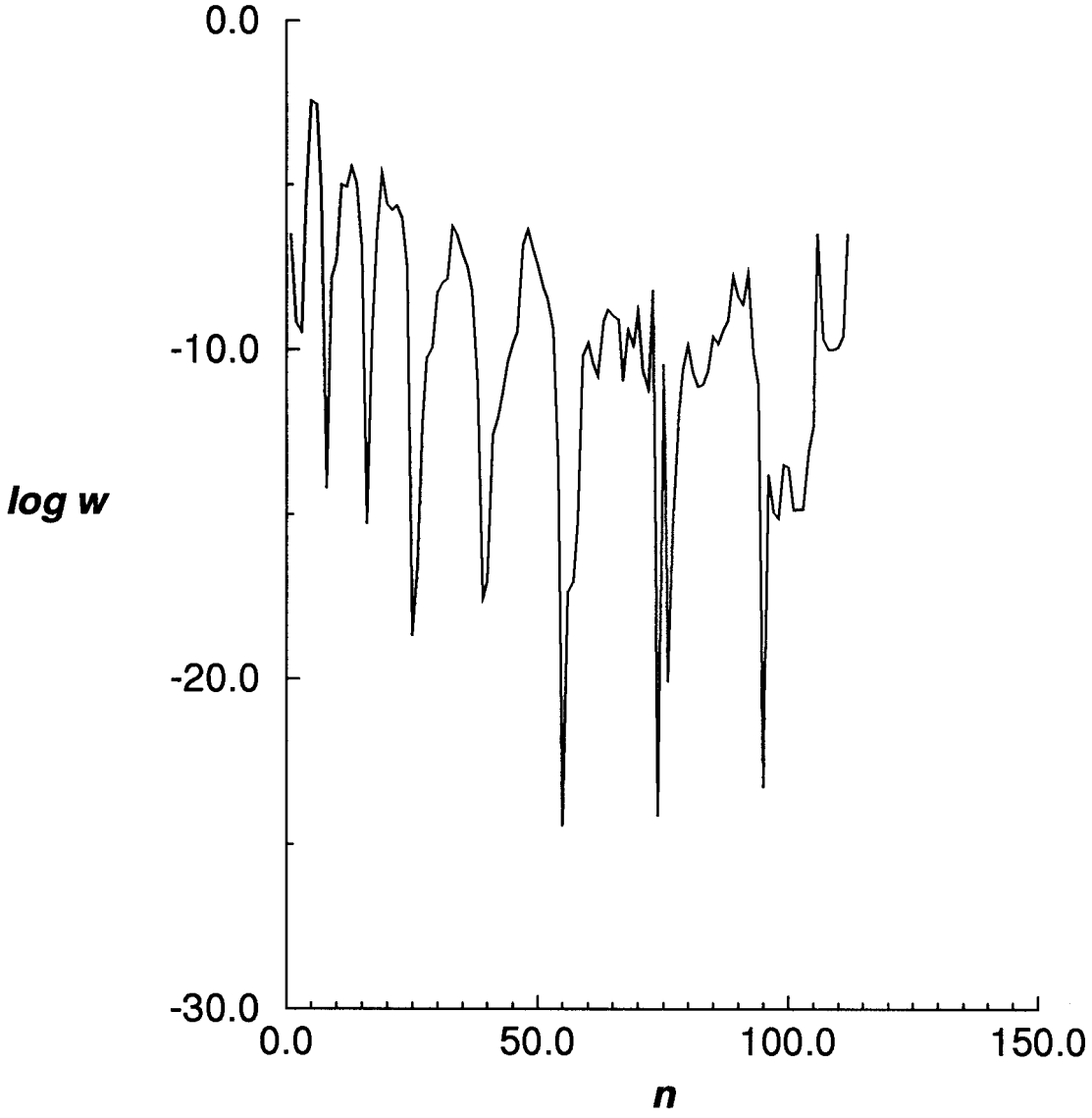

FIG. 9